brief articles

molecular pharmaceutics

Synthesis of Long-Chain [^{18}F]Deoxyfluoropoly(ethylene glycol) Methyl Ethers and Their Noninvasive Pharmacokinetic Analysis by Positron Emission Tomography

Shuji Akai,*,† Sho Ishida,† Kentaro Hatanaka,‡ Takayuki Ishii,‡ Norihiro Harada,§ Hideo Tsukada,§ and Naoto Oku‡

Department of Synthetic Organic Chemistry, Department of Medical Biochemistry, and Global COE Program, Graduate School of Pharmaceutical Sciences, University of Shizuoka, Yada, Suruga-ku, Shizuoka, Shizuoka 422-8526, Japan, and Central Research Laboratory, Hamamatsu Photonics K.K., Hirakuchi, Hamakita-ku, Hamamatsu 434-8601, Japan

Received August 17, 2010; Revised Manuscript Received November 19, 2010; Accepted November 29, 2010

Abstract: [^{18}F]DeoxyfluoroPEG methyl ethers with an average molecular weight of 2 kDa ([^{18}F]**1a**) and 10 kDa ([^{18}F]**1b**) were synthesized by the fluorination of the tosylates **3a**,**b** with [^{18}F]*n*Bu$_4$NF at 80 °C for 20 min followed by flash filtration through a Sep-Pak Plus Alumina-N cartridge. After the intravenous administration of [^{18}F]**1a** and [^{18}F]**1b** to rats, their pharmacokinetics was analyzed by noninvasive, real-time, whole-living-body monitoring using positron imaging technology. The effect of PEG's molecular weight on their blood circulation and organ clearance were quantitatively visualized for the first time.

Keywords: [^{18}F]Deoxyfluoropoly(ethylene glycol) methyl ether; fluorination; pharmacokinetics; poly(ethylene glycol); positron emission tomography

Introduction

Poly(ethylene glycol)s (PEGs) are linear, hydrophilic polyether diols, which are known to be nontoxic and low immunogenic,[1] and eliminated by the combination of renal and hepatic pathways. The covalent attachment of a PEG to a drug or a therapeutic protein, called PEGylation, enhances its stability in blood by protecting it from enzymatic degradation.[2] The PEGylation of drugs also improves their profiles by (1) evading the host immune system, (2) evading the accumulation to a nonspecific tissue, (3) moderating the absorption, and (4) avoiding the renal filtration.[3,4] Therefore, the PEGylation contributes to avoiding the side effects and also to reducing the frequency of administration. In addition, the PEGylation increases the aqueous solubility of poorly soluble drugs.[5] Therefore, the PEGs have been widely employed in pharmaceutical applications.[2,6]

* Corresponding author. Mailing address: University of Shizuoka, Graduate School of Pharmaceutical Sciences, Department of Synthetic Organic Chemistry, Yada, Suruga-ku, Shizuoka, Shizuoka 422-8526, Japan. Tel/fax: +81-54-264-5672. E-mail: akai@u-shizuoka-ken.ac.jp.

† Department of Synthetic Organic Chemistry, Graduate School of Pharmaceutical Sciences, University of Shizuoka.

‡ Department of Medical Biochemistry and Global COE Program, Graduate School of Pharmaceutical Sciences, University of Shizuoka.

§ Central Research Laboratory, Hamamatsu Photonics K.K.

(1) Dreborg, S.; Akerblom, E. B. Immunotherapy with Monomethoxypolyethylene Glycol Modified Allergens. *Crit. Rev. Ther. Drug Carrier Syst.* **1990**, *6*, 315–365.

(2) Greenwald, R. B.; Choe, Y. H.; McGuire, J.; Conover, C. D. Effective Grug Delivery by PEGylated Drug Conjugates. *Adv. Drug Delivery Rev.* **2003**, *55*, 217–250.

(3) Harris, J. M.; Chess, R. B. Effect of Pegylation on Pharmaceuticals. *Nat. Rev. Drug Discovery.* **2003**, *2*, 214–221.

(4) Caliceti, P.; Veronese, F. M. Pharmacokinetic and Biodistribution Properties of Poly(ethylene Glycol)-protein Conjugates. *Adv. Drug Delivery Rev.* **2003**, *55*, 1261–1277.

(5) Veronese, F. M.; Mero, A. The impact of PEGylation on Biological Therapies. *BioDrugs* **2008**, *22*, 315–329.

(6) Knop, K.; Hoogenboom, R.; Fischer, D.; Schubert, U. S. Poly(ethylene Glycol) in Drug Delivery: Pros and Cons As Well as Potential Alternatives. *Angew. Chem., Int. Ed.* **2010**, *49*, 6288–6308.

10.1021/mp100271g
Published on Web 11/29/2010

The PEGylated *Escherichia coli* L-asparaginase (ONCASPAR) is a typical example, which was approved in 1994 by the Food and Drug Administration of the United States for the treatment of acute lymphoblastic leukemia in patients who were hypersensitive to the native unmodified form of L-asparaginase.[7] Some other examples include the PEGylated bovine adenosine deaminase for the treatment of severe combined immunodeficiency associated with ADA deficiency (ADAGEN, 1990),[8,9] the PEGylated antivascular endothelial growth factor RNA aptamer for the treatment of age-related macular degeneration (MACUGEN, 2004),[10,11] and the PEGylated anti-TNF alpha for the treatment of Crohn's disease (CIMZIA, 2008).[12,13] Recently, the PEGylation technology has also been applied to low molecular weight drugs such as camptothecin,[14] irinotecan,[15] and paclitaxel.[16]

For these marketed PEGylated drugs, the PEGs with an average molecular weight (M_w) of 5−40 kDa have been mainly used. The effect of the volume of the PEG moiety on the pharmacokinetics has been investigated based on the *in vitro* and the *in vivo* biological activities of various PEG-drugs[17] and the urinary excretion study of PEG-dicarboxylic acids with different M_ws.[2] Using the ^{125}I-labeled PEGs with different M_ws (6−190 kDa), the distribution and the tissue uptake of the PEGs in mice were also studied.[18] Thereby, it became clear that higher molecular weight PEGs were retained in the blood circulation for a longer period of time than the lower ones, and the urinary and other tissue clearances decreased with the increasing PEG molecular weight, although the real-time, direct trafficking of PEGs in a living body has not been totally achieved.

In this study, [^{18}F]deoxyfluoroPEG methyl ethers with M_w of 2 kDa ([^{18}F]**1a**) and 10 kDa ([^{18}F]**1b**) were synthesized and applied, for the first time, to the detailed pharmacokinetic analysis of rats by planar positron imaging system (PPIS),[19,20] one of the positron imaging technologies, which enabled the noninvasive, real-time, whole-living-body monitoring of the circulation profile, biodistribution and topical accumulation in various tissues, and eventual elimination of **1a** and **1b**. Although there are some [^{18}F]-labeled PEG derivatives with ten ethylene glycol units or less,[21−25] neither the [^{18}F]-labeled PEG with the longer poly(ethylene glycol) chain nor its

(7) Abuchowski, A.; Kazo, G. M.; Verhoest, C. R., Jr.; Van Es, T.; Kafkewitz, D.; Nucci, M. L.; Viau, A. T.; Davis, F. F. Cancer Therapy with Chemically Modified Enzymes. I. Antitumor Properties of Polyethylene Glycol-asparaginase Conjugates. *Cancer Biochem. Biophys.* **1984**, *7*, 175–186.

(8) Nucci, M. L.; Shorr, R.; Abuchowski, A. The Therapeutic Value of Poly(Ethylene Glycol)-Modified Proteins. *Adv. Drug Delivery Rev.* **1991**, *6*, 133–151.

(9) Hershfield, M. S. Adenosine Deaminase Deficiency: Clinical Expression, Molecular Basis, and Therapy. *Semin. Hematol.* **1998**, *35*, 291–298.

(10) Gragoudas, E. S.; Adamis, A. P.; Cunningham, E. T., Jr.; Feinsod, M.; Guyer, D. R. Pegaptanib for Neovascular Age-related Macular Degeneration. *N. Engl. J. Med.* **2004**, *351*, 2805–2816.

(11) Ng, E. W.; Shima, D. T.; Calias, P.; Cunningham, E. T., Jr.; Guyer, D. R.; Adamis, A. P. Pegaptanib, a Targeted Anti-VEGF Aptamer for Ocular Vascular Disease. *Nat. Rev. Drug Discovery* **2006**, *5*, 123–132.

(12) Schreiber, S.; Khaliq-Kareemi, M.; Lawrance, I. C.; Thomsen, O. O.; Hanauer, S. B.; McColm, J.; Bloomfield, R.; Sandborn, W. J. Maintenance Therapy with Certolizumab Pegol for Crohn's Disease. *N. Engl. J. Med.* **2007**, *357*, 239–250.

(13) Schreiber, S.; Rutgeerts, P.; Fedorak, R. N.; Khaliq-Kareemi, M.; Kamm, M. A.; Boivin, M.; Bernstein, C. N.; Staun, M.; Thomsen, O. O.; Innes, A. A Randomized, Placebo-controlled Trial of Certolizumab Pegol (CDP870) for Treatment of Crohn's Disease. *Gastroenterology* **2005**, *129*, 807–818.

(14) Zhao, H.; Lee, C.; Sai, P.; Choe, Y. H.; Boro, M.; Pendri, A.; Guan, S.; Greenwald, R. B. 20-*O*-Acylcamptothecin Derivatives: Evidence for Lactone Stabilization. *J. Org. Chem.* **2000**, *65*, 4601–4606.

(15) Eldon, M. A.; Staschen, C. M.; Viegas, T. X.; Bentley, M. D. NKTR-102, a Novel PEGylated Irinotecan, Results in Sustained Tumor Growth Suppression in Mouse Models of Human Colorectal and Lung Tumors That Correlates with Increased and Sustained Tumor SN38 Exposure. *Mol. Cancer Ther.* **2007**, *6*, 3577s–3578s.

(16) Greenwald, R. B.; Gilbert, C. W.; Pendri, A.; Conover, C. D.; Xia, J.; Martinez, A. Drug Delivery Systems: Water Soluble Taxol 2′-Poly(ethylene Glycol) Ester Prodrugs-design and In Vivo Effectiveness. *J. Med. Chem.* **1996**, *39*, 424–431.

(17) Conover, C. D.; Greenwald, R. B.; Pendri, A.; Shum, K. L. Camptothecin Delivery Systems: The Utility of Amino Acid Spacers for the Conjugation of Camptothecin with Polyethylene Glycol to Create Prodrugs. *Anti-Cancer Drug Des.* **1999**, *14*, 499–506.

(18) Yamaoka, T.; Tabata, Y.; Ikada, Y. Distribution and Tissue Uptake of Poly(ethylene Glycol) with Different Molecular Weights after Intravenous Administration to Mice. *J. Pharm. Sci.* **1994**, *83*, 601–606.

(19) Uchida, H.; Sato, K.; Kakiuchi, T.; Fukumoto, D.; Tsukada, H. Feasibility Study of Quantitative Radioactivity Monitoring of Tumor Tissues Inoculated into Mice with a Planar Positron Imaging System (PPIS). *Ann. Nucl. Med.* **2008**, *22*, 57–63.

(20) Takamatsu, H.; Kakiuchi, T.; Noda, A.; Uchida, H.; Nishiyama, S.; Ichise, R.; Iwashita, A.; Mihara, K.; Yamazaki, S.; Matsuoka, N.; Tsukada, H.; Nishimura, S. An Application of a New Planar Positron Imaging System (PPIS) in a Small Animal: MPTP-Induced Parkinsonism in Mouse. *Ann. Nucl. Med.* **2004**, *18*, 427–431.

(21) Glaser, M.; Morrison, M.; Solbakken, M.; Arukwe, J.; Karlsen, H.; Wiggen, U.; Champion, S.; Kindberg, G. M.; Cuthbertson, A. Radiosynthesis and Biodistribution of Cyclic RGD Peptides Conjugated with Novel [^{18}F]Fluorinated Aldehyde-containing Prosthetic Groups. *Bioconjugate Chem.* **2008**, *19*, 951–957.

(22) Dissoki, S.; Aviv, Y.; Laky, D.; Abourbeh, G.; Levitzki, A.; Mishani, E. The Effect of the [^{18}F]-PEG Group on Tracer Qualification of [4-(Phenylamino)-quinazoline-6-yl]-amide Moiety-An EGFR Putative Irreversible Inhibitor. *Appl. Radiat. Isot.* **2007**, *65*, 1140–1151.

(23) Zhang, W.; Oya, S.; Kung, M. P.; Hou, C.; Maier, D. L.; Kung, H. F. F-18 Polyethyleneglycol Stilbenes as PET Imaging Agents Targeting Aβ Aggregates in the Brain. *Nucl. Med. Biol.* **2005**, *32*, 799–809.

(24) Urakami, T.; Akai, S.; Katayama, Y.; Harada, N.; Tsukada, H.; Oku, N. Novel Amphiphilic Probes for [^{18}F]-Radiolabeling Preformed Liposomes and Determination of Liposomal Trafficking by Positron Emission Tomography. *J. Med. Chem.* **2007**, *50*, 6454–6457.

derivative has yet been reported. Therefore, the successful synthesis of [^{18}F]**1a** and [^{18}F]**1b** is worth noting.

Experimental Section

General. ^{1}H NMR, ^{13}C NMR, and ^{19}F NMR spectra were recorded on a JEOL JMN-ECA-500 (^{1}H, 500 MHz; ^{13}C, 125 MHz; ^{19}F, 470 MHz) instrument with chemical shifts reported in ppm relative to the residual deuterated solvent or the internal standard tetramethylsilane. [^{18}F]-Labeled compounds were synthesized using modified CUPID system (Sumitomo Heavy Industries, Japan). Positron imaging was performed using a planar positron imaging system (PPIS, Hamamatsu Photonics, Japan). This imaging system consists of 2 opposing planar detectors, each having 4 (columns) × 6 (rows) detector units, and each unit composed of 10 × 10 arrays of 2 × 2 × 20 mm^3 pillars of $Bi_4Ge_3O_{12}$ scintillators and a metal packaged position sensitive photomultiplier tube. Focal plane images are constructed from coincidence data collected by opposing planar detectors, achieving data acquisition with higher sensitivity and finer spatial resolution than conventional PET. The radioactivity of the [^{18}F]compound in each organ was measured by a gamma counter, 1480 Wizard (Perkin-Elmer, USA).

Amberlite IR-120 and Amberlite IRA-400 were purchased from Sigma-Aldrich (USA) and activated prior to use as follows: Amberlite IR-120 (10 g), charged in a column, was washed by passing 300 mL of aqueous 1 N HCl over 2 h and then 100 mL of deionized water over 0.5 h. Amberlite IRA-400 was similarly activated using aqueous 1 N NaOH instead of 1 N HCl. The following chemicals were purchased as noted and used without further purification unless otherwise noted: *O*-methylpoly(ethylene glycol) (**2a**, M_w 2 kDa), $Me_3N\cdot HCl$, and nBu$_4$NF (1.0 M THF solution) were purchased from Sigma-Aldrich (USA), *O*-methylpoly(ethylene glycol) (**2b**, M_w 10 kDa) was purchased from HiPep Laboratories (Japan), TsCl was purchased from Kanto Chemical Co., Inc. (Japan), Et_3N was purchased from Kishida Chemical Co., Ltd. (Japan), and an anion-exchange resin AG1-X8 (OH^- form, 100−200 mesh) was purchased from Bio-Rad Laboratories (USA). nBu$_4$NHCO$_3$ was prepared by the reaction of 40% aq nBu$_4$NOH and CO_2. Dehydrated acetonitrile (water content less than 50 ppm) and dehydrated *N*,*N*-dimethylformamide (DMF) (water content less than 50 ppm), both purchased from Wako Pure Chemical Industries, Ltd. (Japan) and Sigma-Aldrich (USA), were used for the fluorination reactions.

***O*-Methyl-*O*-(4-methylbenzenesulfonyl)poly(ethylene glycol) (3a).** Under a nitrogen atmosphere, TsCl (0.57 g, 3.0 mmol) was added to an ice-cold solution of *O*-methylpoly(ethylene glycol) (**2a**, M_w 2 kDa, 1.0 g, 0.50 mmol) and Et_3N (0.47 mL, 3.5 mmol) in anhydrous MeCN (7.5 mL). The reaction mixture was stirred at RT for 10 h and concentrated *in vacuo*. Hexanes (20 mL) were added to the residue, the mixture was stirred at RT for 5 min, and the supernatant was removed by decantation. This process was repeated three times. The residue was dissolved in H_2O−MeCN (1:1, 20 mL), and Amberlite IR-120 (1.0 g) and Amberlite IRA-400 (1.0 g) were added at once. The mixture was vigorously stirred at RT for 20 min and filtered. The ion-exchange resins were rinsed with water (10 mL). The combined rinse solution was concentrated *in vacuo*, and the residue was dried under reduced pressure (<1 mmHg) to give **3a** (0.98 g, 98%) as a colorless solid. ^{1}H NMR (500 MHz, $CDCl_3$): δ 2.41 (3 H, s), 3.34 (3 H, s), 3.45−3.76 (240 H, m), 4.12 (2 H, t, J = 7.5 Hz), 7.31 (2 H, d, J = 8.5 Hz), 7.76 (2 H, d, J = 8.5 Hz).^{13}C NMR (125 MHz, $CDCl_3$): δ 21.5, 58.9, 68.5, 69.1, 70.4, 71.8, 127.9, 129.7, 132.8, 144.7.

***O*-Methyl-*O*-(4-methylbenzenesulfonyl)poly(ethylene glycol) (3b).** Similarly to the preparation of **3a,** a mixture of TsCl (46 mg, 0.24 mmol), **2b** (M_w 10 kDa, 0.40 g, 0.040 mmol), Et_3N (0.055 mL, 0.40 mmol), and $Me_3N\cdot HCl$ (3.8 mg, 0.040 mmol) in anhydrous MeCN (3.0 mL) was stirred at RT for 13 h. Similar purification using ion-exchange resins followed by recrystallization of the crude product from Et_2O−CH_2Cl_2 (10:1) gave **3b** (0.39 g, 98%) as a colorless solid. ^{1}H NMR (500 MHz, $CDCl_3$): δ 2.44 (3 H, s), 3.37 (3 H, s), 3.47−3.77 (1120 H, m), 4.15 (2 H, t, J = 7.5 Hz), 7.33 (2 H, d, J = 8.5 Hz), 7.78 (2 H, d, J = 8.5 Hz). ^{13}C NMR (125 MHz, $CDCl_3$): δ 21.6, 58.9, 68.6, 69.2, 70.5, 71.9, 127.9, 129.8, 133.0, 144.7.

Deoxyfluoropoly(ethylene glycol) Methyl Ether (1a). A solution of **3a** (0.20 g, 0.10 mmol) in anhydrous toluene (2 mL) was concentrated *in vacuo* at RT to remove moisture by azeotropic distillation, and the residue was further dried under reduced pressure (<1 mmHg) at RT for 2 h. The reaction flask was backfilled with nitrogen, and anhydrous DMF (1.0 mL) and nBu$_4$NF (1.0 M THF solution, 0.50 mL, 0.50 mmol) were added in this order. The reaction mixture was stirred at 80 °C for 20 min. After cooling, H_2O−MeOH (1:1, 5.0 mL), Amberlite IR-120 (1.0 g), and Amberlite IRA-400 (1.0 g) were added, and the mixture was vigorously stirred at RT for 20 min and filtered. The ion-exchange resins were rinsed with water (5 mL). The combined rinse solution was concentrated *in vacuo*, and the residue was dried under reduced pressure (<1 mmHg) to give **1a** (0.19 g, 95%) as a colorless solid. ^{1}H NMR (500 MHz, $CDCl_3$): δ 3.37 (3 H, s), 3.49−3.79 (240 H, m), 4.55 (2 H, dt, J = 47, 4.0 Hz),^{13}C NMR (125 MHz, $CDCl_3$): δ 59.0, 70.3, 70.5, 70.8, 71.9, 83.1 (d, J = 168 Hz). ^{19}F NMR (470 MHz, $CDCl_3$): δ −223 (tt, J = 47, 30 Hz).

Deoxyfluoropoly(ethylene glycol) Methyl Ether (1b). Similarly to the preparation of **1a**, a solution of **3b** (50 mg, 5.0 μmol) and nBu$_4$NF (1.0 M THF solution, 0.050 mL, 0.050 mmol) in anhydrous MeCN (0.30 mL) was stirred at 80 °C for 20 min. After similar treatment of the crude product with the ion-exchange resins, the ion-exchange resins were rinsed with H_2O−MeOH (1:1, 10 mL) instead of water. The combined rinse solution was concentrated *in vacuo*, and the

(25) Urakami, T.; Kawaguchi, A. T.; Akai, S.; Hatanaka, K.; Koide, H.; Shimizu, K.; Asai, T.; Fukumoto, D.; Harada, N.; Tsukada, H.; Oku, N. In Vivo Distribution of Liposome-encapsulated Hemoglobin Determined by Positron Emission Tomography. *Artif. Organs* **2009**, *33*, 164–168.

residue was dried under reduced pressure (<1 mmHg) to give **1b** (49 mg, 98%) as a colorless solid. ^{1}H NMR (500 MHz, $CDCl_3$): δ 3.35 (3 H, s), 3.47−3.78 (1120 H, m), 4.55 (2 H, dt, J = 47, 4.0 Hz).^{13}C NMR (125 MHz, $CDCl_3$): δ 59.1, 70.5, 71.9, 83.1 (d, J = 168 Hz). ^{19}F NMR (470 MHz, $CDCl_3$): δ −223 (tt, J = 47, 30 Hz).

[^{18}F]Deoxyfluoropoly(ethylene glycol) Methyl Ether ([^{18}F]1a). [^{18}F]Fluoride was produced using a cyclotron (HM-18, Sumitomo Heavy Industries, Japan) at Hamamatsu Photonics Central Research Laboratory by the ^{18}O(p,n)^{18}F nuclear reaction with [^{18}O]H_2O. [^{18}F]Fluoride was trapped by an anion-exchange resin AG1-X8 and eluted with a 0.15 M solution of nBu$_4$NHCO$_3$ in MeCN (0.5 mL) from the resin. Water was removed by azeotropic distillation by flowing He (200 mL/min) at 110 °C for 12 min. The addition of MeCN (1 mL) to the residue and the subsequent azeotropic distillation were repeated twice. Then, the residue was dried under reduced pressure for 1 min, and the reaction vessel was purged with He flow (200 mL/min) for 1 min to ensure complete dryness. Finally, the reaction vessel was cooled to RT, and DMF (0.5 mL) was added to make a solution of [^{18}F]nBu$_4$NF for the following radiolabeling. The precursor **3a** was subjected to the azeotropic distillation of its toluene solution at RT followed by dryness under reduced pressure (<1 mmHg) for 2 h to remove moisture. **3a** (5.0 mg, 2.5 μmol) was added to the above-mentioned solution of [^{18}F]nBu$_4$NF in DMF. The mixture was heated at 80 °C for 20 min. After cooling, the reaction mixture was filtered through a Sep-Pak Plus Alumina-N cartridge with water to give [^{18}F]**1a**, whose radiochemical purity was determined to be 96% by the radio-TLC analysis of the crude product.

[^{18}F]Deoxyfluoropoly(ethylene glycol) Methyl Ether ([^{18}F]1b). Similarly to the preparation of [^{18}F]**1a**, [^{18}F]**1b** was prepared using **3b** (0.10 g, 0.010 mmol) in MeCN (0.6 mL) instead of DMF as the reaction solvent. The radiochemical purity of [^{18}F]**1b** was determined to be 95% by the radio-TLC analysis of the crude product.

Whole-Body Biodistribution Analysis of [^{18}F]1a and [^{18}F]1b in Rats. Seven-week-old male Wistar rats weighing 180−220 g were obtained from Japan SLC (Shizuoka, Japan). Rats were maintained and handled with the recommendations of the National Institutes of Health, the Guidelines of the University of Shizuoka, and the Guidelines of the Central Research Laboratory, Hamamatsu Photonics. Kinetics and distribution patterns of the [^{18}F]-labeled PEGs were determined with the PPIS. The animals were anesthetized with an intraperitoneal injection of chloral hydrate at 50 mg/kg and were fixed prone on an acrylic plate. The plate was placed on the midplane between the two opposing detectors arranged in a horizontal mode. A solution of [^{18}F]**1a** or [^{18}F]**1b** in 0.5 mL of saline (5.0 MBq/rat) was intravenously administered to rats via the tail vein. The data were acquired with a 1 min frame for 60 min, and summation images were created every 10 min. Images were analyzed using software, Image J, and displayed as 109 × 169 pixels. These experiments were repeated at least three times in which similar results were obtained. Typical results obtained from a single animal are shown in Figure 2. Time−activity curves of ^{18}F in heart, kidney, and bladder were obtained from the mean pixel radioactivity in the region of interest (ROI) of the PPIS images (Figure 3), where the injected dose was calibrated as 5 MBq and the percent of injected dose per gram tissue was calculated based on the weight of each tissue obtained from the following experiment.

Determination of Organ Distribution. Rats injected with the [^{18}F]-labeled PEG were killed by decapitation under Et_2O anesthesia immediately after PPIS scanning for 60 min. The blood was collected from the carotid artery, and its total volume was assumed to be 6.41% of the body weight. Samples of heart, lung, liver, spleen, and kidney were rapidly isolated and weighed. The radioactivity of the [^{18}F]compounds in liver and kidney was determined by measuring a portion of the shattered organ using a gamma counter, while that in heart, lung, and spleen was determined by measuring the whole organ.

Results

Chemistry. We started this project by examining the fluorination of a commercially available PEG methyl ether **2a** (M_w 2 kDa). At first, the corresponding tosylate **3a**, a substrate of the fluorination, was prepared by the standard method using TsCl and Et_3N.[26] Because **2a** was a mixture of dozens of PEGs with different lengths of the ethylene glycol units, TLC analysis could not effectively monitor the reaction. In contrast, we found that the 500 MHz ^{1}H NMR analysis of a crude reaction mixture was very convenient for obtaining quantitative information. The purification of **3a** was another concern. Typical purification methods, such as washing with water and organic solvents, crystallization,[27] and column chromatography, were less useful and/or required laborious work due to the high polarity and high solubility of **3a** in both organic solvents and water. In particular, these methods could hardly eliminate excess amounts of the reagents and side products, such as $Et_3N\cdot$TsOH, from the crude products. On the other hand, treatment with a strongly acidic cation exchange resin, Amberlite IR-120, and a strongly basic anion exchange resin, Amberlite IRA-400, successfully eliminated these impurities to give pure **3a** in 98% yield (Scheme 1).

Because of the fairly short half-life (110 min) of ^{18}F, the substitution of **3a** with a [^{18}F]fluoride ion needed to be completed in a short time. To find suitable conditions, preliminary experiments were conducted using 1.0 equiv of three kinds of cold fluorides, KF-Kryptofix[2.2.2], CsF, and nBu$_4$NF, in various polar organic solvents (0.10 M) at 80 °C. The time course of each reaction was monitored by the direct ^{1}H NMR analysis of a small portion of the reaction

(26) Harris, J. M.; Struck, E. C.; Case, M. G.; Paley, M. S.; Vanalstine, J. M.; Brooks, D. E. Synthesis and Characterization of Poly(Ethylene Glycol) Derivatives. *J. Polym. Sci.: Polym. Chem. Ed.* **1984**, *22*, 341–352.

(27) Li, J.; Kao, W. J. Synthesis of Polyethylene Glycol (PEG) Derivatives and PEGylated-peptide Biopolymer Conjugates. *Biomacromolecules* **2003**, *4*, 1055–1067.

Scheme 1[a]

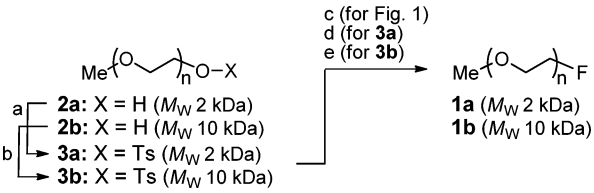

[a] Reagents and conditions: (a) TsCl (6.0 equiv), Et_3N (7.0 equiv), MeCN, 0 °C to RT, 10 h, then Amberlite IR-120/Amberlite IRA-400; (b) TsCl (6.0 equiv), Et_3N (10 equiv), $Me_3N{\cdot}HCl$ (1.0 equiv), MeCN, 0 °C to RT, 13 h, then Amberlite IR-120/Amberlite IRA-400; (c) fluoride ion (1.0 equiv), organic solvent (0.10 M), 80 °C; (d) nBu$_4$NF (5.0 equiv), DMF, 80 °C, 20 min, then Amberlite IR-120/Amberlite IRA-400; (e) nBu$_4$NF (10 equiv), MeCN, 80 °C, 20 min, then Amberlite IR-120/Amberlite IRA-400.

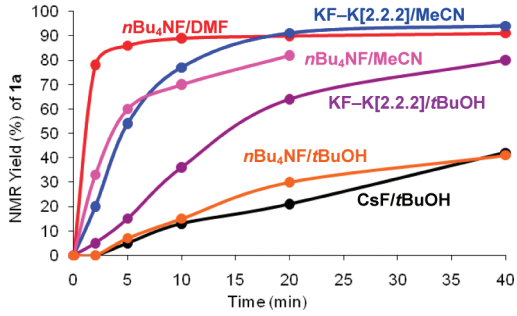

Figure 1. Time course of the fluorination of **3a** under various conditions.

mixture in D_2O (Figure 1). Some results are worthy of note: (1) The use of KF-Kryptofix[2.2.2] in MeCN, which was effectively used in our previous synthesis of the PET probes for liposomal trafficking,[24,25] provided the fluorinated PEG **1a** (90% NMR yield) after 20 min. (2) The use of *t*BuOH as a reaction medium was reported to enhance the reactivity of CsF or nBu$_4$NF and reduce the formation of side products;[28] however, it was not suitable in our case. (3) The use of nBu$_4$NF in DMF was the best among all the conditions we examined, which gave **1a** (90% NMR yield) within 10 min.

For the practical preparation of **1a**, **3a** was reacted with nBu$_4$NF (5.0 equiv) in DMF (0.10 M) at 80 °C for 20 min, and the crude reaction mixture was treated with a mixture of Amberlite IR-120 and Amberlite IRA-400 to afford **1a** in 95% isolated yield (Scheme 1).

The preparation of the fluoride **1b** (M_w 10 kDa) from the commercially available PEG **2b** (M_w 10 kDa) was attained with some modification. While the tosylation of **2b** under similar conditions gave an approximately 70% yield of **3b** after 24 h, the addition of an equivalent amount of $Me_3N{\cdot}HCl$[29] to the above-mentioned conditions significantly accelerated the reaction to give **3b** in more than 95% yield

Scheme 2[a]

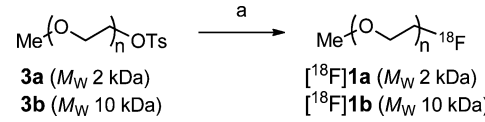

[a] Reagents and conditions: (a) [^{18}F]nBu$_4$NF, DMF (for **3a**), MeCN (for **3b**), 80 °C, 20 min, then Sep-Pak Plus Alumina-N cartridge.

after 13 h. The fluorination of **3b** was successfully carried out using nBu$_4$NF (1.0 equiv) in MeCN at 80 °C for 20 min followed by a treatment with the ion exchange resins to give **1b** (M_w 10 kDa) in 77% yield, although a similar reaction in DMF was less effective. A 98% yield of **1b** was obtained using 10 equiv of nBu$_4$NF in MeCN (Scheme 1).

With the effective fluorination conditions in hand, we next examined the reaction with [^{18}F]nBu$_4$NF. The [^{18}F]fluoride ion, generated by a cyclotron, was trapped by an anion-exchange resin AG1-X8 and eluted with nBu$_4$NHCO$_3$ in MeCN to form a solution of [^{18}F]nBu$_4$NF in MeCN, which was concentrated by flowing He at 110 °C. DMF was added to make a solution of [^{18}F]nBu$_4$NF, and **3a** was added. The reaction mixture was heated at 80 °C for 20 min, then filtered through a Sep-Pak Plus Alumina-N cartridge with water to give the desired [^{18}F]**1a**. A similar reaction of **3b** with [^{18}F]nBu$_4$NF in MeCN at 80 °C for 20 min followed by purification afforded [^{18}F]**1b** (Scheme 2).

Pharmacokinetic Analysis. Seven-week-old male Wistar rats weighing 180−220 g were used for the pharmacokinetic analysis of the [^{18}F]-labeled PEGs ([^{18}F]**1a** and [^{18}F]**1b**). The animals were anesthetized with an intraperitoneal injection of chloral hydrate, fixed on an animal holder, and then intravenously injected with a single dose of [^{18}F]**1a** or [^{18}F]**1b** in saline (5.0 MBq/rat) via the tail vein. The PPIS scan was started immediately after the administration and performed for 60 min, and images were analyzed using software, Image J, and displayed as 109 × 169 pixels (Figure 2). A time−activity curve was obtained from the mean pixel radioactivity in the region of interest (ROI) of the PPIS images where the injected dose was calibrated as 5 MBq (Figure 3). At 60 min after the administration, the rats were immediately sacrificed under anesthesia to collect the blood from the carotid artery. The radioactivity of [^{18}F]**1a** and [^{18}F]**1b** in blood and several dissected organs was measured by a gamma counter (Figure 4).

Discussion and Conclusion

We have succeeded in the preparation of the [^{18}F]deoxyfluoroPEGs with M_w of 2 kDa and 10 kDa via the nucleophilic substitution of the hydroxyl group of PEGs with a [^{18}F]fluoride ion. The suitable choice of the reaction solvents (DMF and

(28) Kim, D. W.; Jeong, H. J.; Lim, S. T.; Sohn, M. H.; Katzenellenbogen, J. A.; Chi, D. Y. Facile Nucleophilic Fluorination Reactions Using *tert*-Alcohols as a Reaction Medium: Significantly Enhanced Reactivity of Alkali Metal Fluorides and Improved Selectivity. *J. Org. Chem.* **2008**, *73*, 957–962.

(29) Yoshida, Y.; Sakakura, Y.; Aso, N.; Okada, S.; Tanabe, Y. Practical and Efficient Methods for Sulfonylation of Alcohols Using Ts(Ms)Cl/Et_3N and Catalytic $Me_3N{\cdot}HCl$ as Combined Base: Promising Alternative to Traditional Pyridine. *Tetrahedron* **1999**, *55*, 2183–2192.

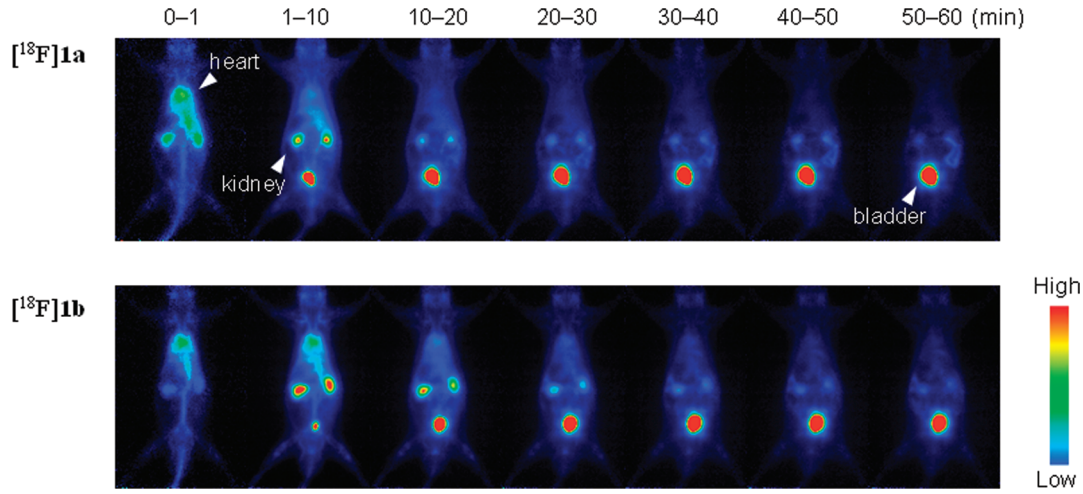

Figure 2. PPIS imaging with [^{18}F]**1a** (top) and [^{18}F]**1b** (bottom). A solution of [^{18}F]**1a** or [^{18}F]**1b** in 0.5 mL of saline (5.0 MBq/rat) was intravenously administered to Wistar rats via the tail vein. Images were acquired with a 1 min frame, and the accumulated data for every 10 min are shown.

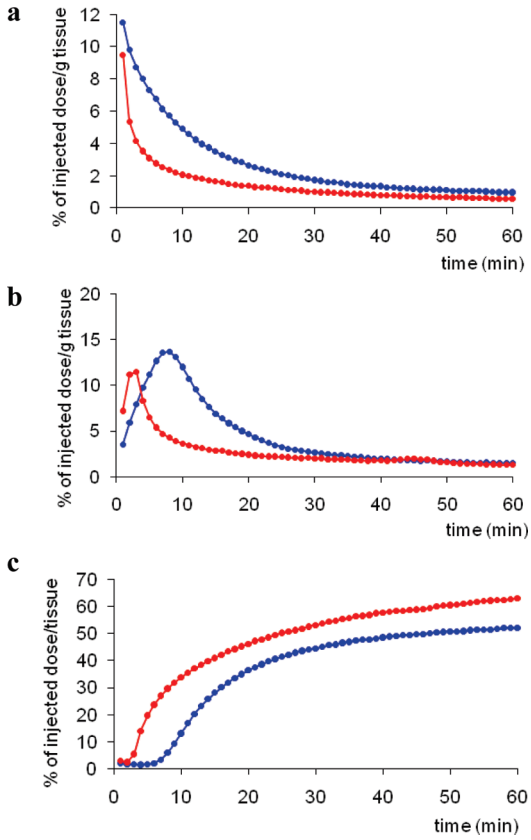

Figure 3. Real-time changes in ROI of the PPIS images with [^{18}F]**1a** (2 kDa, red) and [^{18}F]**1b** (10 kDa, blue). The time−activity curves of ^{18}F in heart (a), kidney (b), and bladder (c) were obtained from the mean pixel radioactivity in ROI of the PPIS images acquired with a 1 min frame after the administration.

MeCN), a fluoride source (nBu$_4$NF), and the temperature (80 °C) was the key to achieve rapid synthesis within 20 min. This fluorination method is basically applicable to the PEGs with higher molecular weight such as M_w 20 kDa. However, along with the increasing molecular weight, the significant decrease of the reactivity and the increase of the viscosity become serious

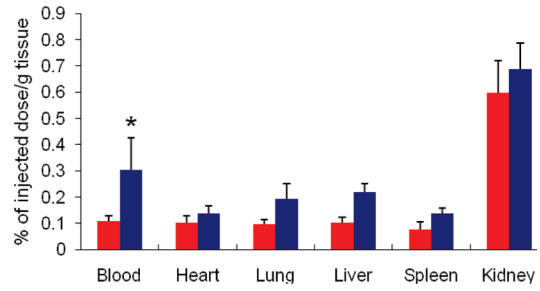

Figure 4. Biodistribution of [^{18}F]**1a** (2 kDa, red) and [^{18}F]**1b** (10 kDa, blue) in blood and several organs dissected 60 min after the administration. The radioactivity of the [^{18}F]compound in each organ was measured by a gamma counter. Data are presented as the mean ± SD (n = 4). Significant differences from the [^{18}F]**1a** group are indicated (*P < 0.05).

issues. We are now addressing the improvement of the procedure to overcome these problems.

The real-time translocation of the long-chain PEGs, [^{18}F]**1a** (M_w 2 kDa) and [^{18}F]**1b** (M_w 10 kDa), from heart to liver, kidney, and then bladder was noninvasively and clearly visualized by PPIS for the first time (Figure 2). The movement of [^{18}F]**1b** was slower than that of [^{18}F]**1a**, and differences were observed between 0 and 30 min. The ROI of the PPIS images on the heart, kidney, and bladder (Figure 3) also demonstrated the minute variations in the concentrations of [^{18}F]**1a** and [^{18}F]**1b** in each organ. A typical result is that [^{18}F]**1a** accumulated in kidney within 3 min after the administration and rapidly transferred to bladder, while the accumulation of [^{18}F]**1b** in kidney reached a maximum in 8 min, and then it was moderately transferred to the bladder. It was also indicated that half of [^{18}F]**1a** or [^{18}F]**1b** was excreted after approximately 25 and 50 min, respectively. The effect of the PEG's molecular weight on their blood circulation and organ clearances also became apparent by the direct analysis of the collected blood and the dissected organs (Figure 4).

Ikada et al. investigated the biodistribution and the tissue uptake of PEGs with different molecular weights (M_w 6−190 kDa) after their intravenous administration to mice.[18] They synthesized ^{125}I-labeled PEGs by connecting tyramine to terminal hydroxyl groups of the PEGs using carbonyl diimidazole, followed by the radioiodination of the installed tyramine residues. The radioactivity of the collected blood, the dissected organs, and the carcass was measured by a gamma counter. They reported that higher molecular weight PEGs were retained in the blood circulation for a longer period of time than the lower ones. On the other hand, Greenwald et al. published the urinary excretion study of PEG-dicarboxylic acids with different molecular weights (M_w 8−40 kDa) in rats following intravenous administration.[2] They verified an inverse correlation between the M_w and excretion rate. In our experiments, [^{18}F]**1b** (M_w 10 kDa) was retained in the blood at higher concentration than [^{18}F]**1a** (M_w 2 kDa), and the former was less readily excreted from kidney than the latter. There was also a difference in their translocation to the bladder. These results are consistent with the reported pharmacokinetics of various PEGs.[2,18]

One of the major advances of this study is the successful application of positron imaging technology, which enables the noninvasive, real-time, precise monitoring of the PEGs in a whole-living-body as well as some typical organs.

In summary, the present study has revealed the detailed pharmacokinetics of two kinds of long-chain deoxyfluoroPEGs, [^{18}F]**1a** (M_w 2 kDa) and [^{18}F]**1b** (M_w 10 kDa), in living rats for the first time. It was achieved by the successful synthesis of [^{18}F]deoxyfluoroPEGs by nucleophilic substitution of the hydroxyl group of the PEGs with a [^{18}F]fluoride ion. The rapid reaction (20 min) of such high molecular weight PEGs with a less nucleophilic fluoride ion is of particular note. The remarkable advantages of positron imaging technology such as PET and PPIS on the biodistribution analysis of the PEGs has also been demonstrated on the basis of the spatiotemporal and quantitative data. Extensive applications of the developed methodology for PEGylated drugs and drug candidates are currently under investigation.

Abbreviations Used

DMF, *N*,*N*-dimethylformamide; M_w, average molecular weight; PEG, poly(ethylene glycol); PET, positron emission tomography; PPIS, planar positron imaging system; ROI, region of interest; RT, room temperature; TNF, tumor necrosis factor; Ts, *p*-toluenesulfonyl; TsCl, *p*-toluenesulfonyl chloride.

Acknowledgment. This study was financially supported by a Grant-in-Aid for the Global COE Program from MEXT. We thank Dr. T. Kakiuchi, Mrs. H. Uchida and K. Sato at Hamamatsu Photonics K.K. for their technical assistance in the PPIS study.

Supporting Information Available: NMR data for all new compounds. This material is available free of charge via the Internet at http://pubs.acs.org.

MP100271G